

# Correlated magnetic noise from anisotropic lightning sources and the detection of stochastic gravitational waves

Yoshiaki Himemoto<sup>1</sup> and Atsushi Taruya<sup>2,3</sup>

<sup>1</sup>*Department of Liberal Arts and Basic Sciences, College of Industrial Technology,  
Nihon University, Narashino, Chiba 275-8576, Japan*

<sup>2</sup>*Center for Gravitational Physics, Yukawa Institute for Theoretical Physics, Kyoto University, Kyoto 606-8502, Japan*

<sup>3</sup>*Kavli Institute for the Physics and Mathematics of the Universe,  
Todai Institutes for Advanced Study, the University of Tokyo,  
Kashiwa, Chiba 277-8583, Japan (Kavli IPMU, WPI)*

(Dated: May 14, 2022)

Direct detection of gravitational waves (GW) from compact binary systems suggests that the merger rate of such events is too large to be individually resolved, and thus they can be detected as stochastic signals. Due to its random nature, cross-correlating the signals from multiple detectors is essential to disentangle the GWs from instrumental noise. However, the global magnetic fields in the Earth-ionosphere cavity produce the environmental disturbances at low-frequency bands, known as Schumann resonances, and coupled with GW detectors, they potentially contaminate the stochastic GW signal as a correlated noise. Previously, we have presented a simple analytical model to estimate its impact on the detection of stochastic GWs. Here, extending the analysis to further take account of the effects of anisotropic lightning source distributions, we present a comprehensive study of the impact of correlated magnetic noise at low-frequency bands, including non-tensor type GWs, as well as circularly polarized tensor-type GWs. We find that as opposed to a naive expectation, the impact of correlated magnetic noise does not always increase with anisotropies in the lightning source distribution. Even in the presence of large anisotropies, there is a robust detector pair for which the amplitude of correlated magnetic noise becomes comparable to or well below detectable amplitude of stochastic GWs. The results indicate that the properties of the correlated magnetic noise depends crucially on both the geometrical and geographical setup of detector's pair, and Virgo and KAGRA would be potentially the most insensitive detector pair against the correlated magnetic for both tensor- and non-tensor type stochastic GWs.

## I. INTRODUCTION

Since the first discovery of gravitational wave (GW) event by laser interferometer LIGO (Hanford and Livingston, [1, 2]), there is a growing interest in detecting the stochastic gravitational wave backgrounds. Stochastic GWs are basically produced by an incoherent superposition of an extremely large number of GWs from the unresolved astrophysical sources and/or high-energy cosmological phenomena such as inflation, cosmic strings, and phase transitions (For a review, see e.g., [3]). In particular, recent detections of compact binary coalescences [4–9] suggest that the expected number of such events over the cosmological scales would be too large to be individually resolved, and low signal-to-noise ratio events can contribute to the stochastic GW, which would be potentially detectable with currently operating ground-based detectors [10] (see also [11–16]).

There are, however, several concerns and issues toward a decisive detection of stochastic GWs. One of the most serious concerns is the contamination by the correlated environmental noise between detectors. Due to the random nature of the signal, a detection of stochastic GW is made possible by taking a cross correlation between the data streams obtained from the multiple set of detector. This cross correlation technique offers a way to isolate the stochastic GW signals from detector's noise if the noises are totally uncorrelated. It has been pointed out,

however, by Refs. [17, 18] that the correlated noise arises from the (stationary) global electromagnetic fields on the Earth, known as Schumann resonances [19, 20], through the coupling with magnets or magnetically susceptible materials in the laser interferometer system. Such a correlated noise can also give an impact on searches for transient GW events [21].

There are thus several experimental and theoretical studies to estimate the impact of correlated noise, and a technique to mitigate its impact has been also proposed in Refs. [22–24]. While the recent study suggests that the correlated noise budget including the one arising from the Schumann resonance is less significant and ignorable at LIGO detectors [25], the potential impact still remains at other detector sites, and a clear signal of Schumann resonances has been indeed detected through the magnetometer measurements between Virgo [26] and KAGRA [27] sites [28].

In this respect, we have recently presented a simple analytical model to estimate the impact of correlated magnetic noise [24]. The model reproduces the major trend of the measured global correlation between the GW detectors via magnetometer, and the estimated value of the impact of correlated noise quantitatively match those inferred from the measurement results. Then, as an implication, we have explored the possible impact of the correlated noise on the detection of stochastic GWs from existing four detectors and planned detector, LIGO In-

dia [29], finding that in the pessimistic case that most of the detector pairs are completely dominated by the correlated noise, LIGO Hanford-Virgo and Virgo-KAGRA pairs would be possibly less sensitive to the correlated noise, and may achieve the best sensitivity to the stochastic GWs.

While the analytic model in our previous paper shows several interesting properties, and can be even used to quantitatively estimate the impact of correlated noises, several simplifications made in the model needs to be verified and/or scrutinized for a proper modeling of the correlated magnetic noise. Apart from the non-stationarity of the Schumann resonances, one potentially important effect may be the inhomogeneous distribution of the exciting sources of global magnetic fields, which can result in the anisotropies of the magnetic field spectrum. Although our previous study simply assumed the isotropic distribution of exciting sources, the lightning sources are in reality associated with global weather activity, and these are known to concentrate on the continental areas in the tropics. Indeed, the time variation of Schumann resonances measured at widely-separated radio station clearly suggests the inhomogeneous distribution of exciting sources for magnetic fields [30, 31]. The anisotropic magnetic field induced by the inhomogeneous lightning distribution may alter the correlated properties of magnetic noises, and can add another impact on the detection of stochastic GWs.

Primary purpose of this paper is to present a comprehensive study of the impact of correlated magnetic noise on the detection of stochastic GWs, taking the anisotropic distribution of lightning sources into consideration. For this purpose, we extend our analytical model to include the anisotropies in the magnetic field spectrum. Meanwhile, the impact of the correlated magnetic noise crucially depends on the underlying assumption of GWs. While we previously focused on the unpolarized tensor GWs, there may be possibility to have non-standard polarization modes, and the detection of such GWs would be important. We will thus discuss quantitatively how the correlated magnetic noise can give an impact on the detectability of non-standard GWs.

This paper is organized as follows. In Sec. II, after briefly reviewing the cross correlation analysis, we introduce the analytical model that has been proposed in our previous paper. In Sec. III, taking the anisotropies in the lightning source distribution seriously, we consider an extension of our analytical model, and discuss its potential impact on the detection of stochastic GWs. Sec. IV then presents quantitative estimation of the impact of correlated magnetic noise. Based on the observed spatial distribution of lightning activities, we evaluate the size of correlated magnetic noise for each pair of ongoing and upcoming second-generation GW detectors, and examine how the presence of anisotropies in the lightning source distribution, or equivalently the magnetic field spectrum can change the results, depending on which types of GW we observe. In Sec. V, to understand the behav-

iors seen in previous section, we consider somewhat artificial setup, and discuss the geographical dependence of the impact of correlated magnetic noise. Finally, Sec. VI presents a summary of our important findings and conclusion.

## II. CROSS CORRELATION ANALYSIS IN THE PRESENCE OF CORRELATED MAGNETIC NOISE

In this section, we begin by briefly reviewing the standard cross correlation analysis. We then consider the correlated magnetic noise, and introduce an analytical model presented in Ref. [24] that describes the coherence properties of the magnetic noise.

### A. cross correlation analysis

Let us first denote the time-series output data at  $i$ -th detector by

$$s_i(t) = h_i(t) + n_i(t), \quad (1)$$

where  $h_i$  is the strain amplitude produced by stochastic GWs and  $n_i$  is the noise strain. Since the signal of stochastic GWs is supposed to be very weak and have random properties, it is hard to distinguish between the GW signals and instrumental noise only with a single detector. One way to discriminate the GW signal from the noise is to use multiple set of detectors and to cross-correlate between the output data.

Given the two output data with the observation time of  $T$ , we define the cross correlation statistic  $S$  as

$$S = \int_{-T/2}^{T/2} dt \int_{-T/2}^{T/2} dt' s_1(t) s_2(t') Q(t-t'). \quad (2)$$

Here, the filter function  $Q$  is introduced to enhance the detectability of the GW signals, and its explicit form will be given later as the Fourier transform  $\tilde{Q}$  [see Eq. (8)].

Consider first the case that the noises between two detectors are statistically uncorrelated. The expectation value of the statistic  $S$  then leads to

$$\langle S \rangle = \langle S_G \rangle, \quad (3)$$

with  $\langle S_G \rangle$  given by

$$\langle S_G \rangle \equiv \int_{-T/2}^{T/2} dt \int_{-T/2}^{T/2} dt' \langle h_1(t) h_2(t') \rangle Q(t-t'). \quad (4)$$

Assuming that the support of the filter function in the time domain is small enough compared to the observation time, it is expressed in the Fourier domain as (e.g., [18, 32])

$$\langle S_G \rangle = \frac{3H_0^2}{10\pi^2} T \int_0^\infty df f^{-3} \sum_A \Omega_{\text{gw}}^A(f) \gamma_{12}^A(f) \tilde{Q}(f), \quad (5)$$

where  $H_0 = 100 h \text{ km s}^{-1} \text{ Mpc}^{-1}$  is the Hubble parameter and the function  $\tilde{Q}$  is the Fourier transform of the optimal filter function. Here, summation with respect to  $A$  runs over the polarization modes of GWs. The quantity  $\Omega_{\text{gw}}^A$  is the normalized logarithmic energy density of the stochastic GWs, and  $\gamma_{12}^A$  is the overlap reduction function which represents the coherence of the gravitational strains between the two separated detectors.

In general relativity, tensor mode is only allowed for polarization mode of GWs, but it would be possible in general metric theory of gravity to have additional polarization modes, i.e., vector and scalar modes (e.g., [33–35]). A measurement of vector and/or scalar polarizations thus offers an important test of general relativity. In this paper, we consider the vector and scalar modes, assuming that these are unpolarized. For the tensor modes, we examine both the unpolarized and circularly polarized GWs, as the possibility to generate polarized GWs has been pointed out by several works [36, 37]. Detectability of the stochastic GWs for unpolarized vector/scalar modes and the circularly polarized tensor mode has been previously studied in both ground- and space-based detectors (see e.g., [32, 38] for unpolarized vector and scalar modes, [39–41] for circularly-polarized tensor mode).

In the weak-signal limit (i.e.  $|h_i| \ll |n_i|$ ), in contrast to  $S$ , dispersion of the cross correlation statistic  $S$ , defined by  $\sigma^2 \equiv \langle S^2 \rangle - \langle S \rangle^2$ , is dominated by detector's noise. Thus, one can define the signal-to-noise ratio of the measured stochastic GWs as

$$\text{SNR}_G \equiv \frac{\langle S_G \rangle}{\sigma}. \quad (6)$$

Under the assumption that noises follow the Gaussian statistics, the quantity  $\sigma$  is expressed as

$$\sigma^2 \simeq \frac{T}{2} \int_0^\infty df P_1(f) P_2(f) |\tilde{Q}(f)|^2, \quad (7)$$

where the function  $P_i$  is the instrumental noise spectrum for  $i$ -th detector. Maximizing the signal-to-noise ratio then lead to the optimal filter in the following form [18]:

$$\tilde{Q}(f) \propto \frac{\sum_A \Omega_{\text{gw}}^A(f) \gamma_{12}^A(f)}{f^3 P_1(f) P_2(f)}. \quad (8)$$

Provided the template of stochastic GW spectrum  $\Omega_{\text{gw}}^A$ , Eq. (6) quantifies the statistical significance of measured GW signals. However, the crucial assumption in the standard cross correlation analysis is that the noises are statistically uncorrelated. In what follows, we consider the situation that mirror control system in the laser interferometers is coupled to the global magnetic fields in the Earth-ionosphere cavity to some extent, and this leads to a certain amount of statistically correlated noises.

Let us decompose the strain amplitude of the noise  $n_i$  in Eq. (1) into two pieces:

$$n_i(t) = n_i^I(t) + n_i^B(t). \quad (9)$$

Here,  $n_i^I(t)$  is the instrumental noise originated from local disturbances, and  $n_i^B(t)$  represents the correlated noise induced by the global magnetic fields on the Earth. In the presence of second term, the expectation value of the cross correlation statistic becomes  $\langle S \rangle = \langle S_G \rangle + \langle S_B \rangle$  with  $\langle S_B \rangle$  given by

$$\langle S_B \rangle = \int_{-T/2}^{T/2} dt \int_{-T/2}^{T/2} dt' \langle n_1^B(t) n_2^B(t') \rangle Q(t-t'). \quad (10)$$

Since the coupling between the mirror control system and the global magnetic field is supposed to be small, we may consider that the correlated noise  $n_i^B$  is linearly proportional to the global magnetic field  $B^a$  at  $i$ -th detector's position,  $\mathbf{x}_i$ . Then, the correlated noise is generally expressed in terms of quantities in the Fourier domain as follows:

$$\tilde{n}_i^B(f) = r_i(f) \left[ \hat{\mathbf{X}}_i \cdot \tilde{\mathbf{B}}(f, \mathbf{x}_i) \right]. \quad (11)$$

Here, the frequency-dependent quantity  $r_i$  is called the transfer function, which characterizes the strength of the coupling between the detector and magnetic field, and the unit vector  $\hat{\mathbf{X}}_i$  describes the directional dependence of its coupling. With Eq. (11), the expectation value  $\langle S_B \rangle$  is rewritten in terms of the quantities in the Fourier domain with

$$\langle S_B \rangle = T \int_0^\infty df \text{Re} [r_1^*(f) r_2(f) M_{12}(f)] \tilde{Q}(f), \quad (12)$$

where the function  $M_{12}$  is the correlated magnetic noise spectrum for a pair of detector, given by

$$M_{12}(f) = \hat{X}_{1,a} \hat{X}_{2,b} \langle \tilde{B}^{a*}(f, \mathbf{x}_1) \tilde{B}^b(f, \mathbf{x}_2) \rangle', \quad (13)$$

where the prime in  $\langle \dots \rangle'$  denotes that we removed the delta function  $\delta_D(f - f')$ . The labels  $a, b$  run from 1 to 3.

$M_{12}$  is one of the important quantities that determines the magnitude of the correlated noise, and as pointed out in Ref. [24], this quantity depends not only on the strength and propagation of magnetic fields, but also on the coherence of the response of the two separated detectors to the magnetic fields. In next subsection, we present a simple analytical model of  $M_{12}$  in Ref. [24].

## B. Correlated magnetic noise spectrum

To investigate further the impact of correlated magnetic noise, we follow Ref. [24], and consider a simple analytical model. Note that even with simplified setup, the model captures several important properties of correlated magnetic noise that have been partly observed through the measurement with magnetometers [22, 23]. The basic assumptions of the model are summarized as follows:

1. The magnetic noise spectrum describes the frequency-dependent coherence of the global magnetic field between two detectors, which is expressed as a sum of the discrete Schumann resonance modes convolving the line-shape function. Here, the Schumann resonances are idealistically represented by a superposition of the axisymmetric TM modes of the Earth-ionosphere cavity with respect to each exciting source [42].
2. The TM modes are generated by lightning sources which are produced continuously in a stationary random process. That is, the amplitude of TM mode,  $\tilde{B}$ , has a random nature, and is characterized by the power spectrum, which is the function of angular position of lightning source  $\hat{\Omega}$  and frequency  $f$ . For simplicity, we further assume that the lightning distribution is isotropic.

Based on the above assumptions, the explicit expression for the correlated magnetic noise spectrum  $M_{12}$  is given by Ref. [24]

$$M_{12}(f) = \frac{1}{8\pi} P_B(f) \sum_{\ell} \frac{|E_{\ell}(f)|^2}{|E_{\ell}(f_{\ell})|^2} \gamma_{\ell}^B(\hat{\mathbf{r}}_1, \hat{\mathbf{r}}_2). \quad (14)$$

Here,  $P_B$  is the (single-sided) power spectrum density of the magnetic field, and is defined through the ensemble average of the amplitude of the TM mode  $\tilde{B}$ , given by (assuming isotropic distribution)

$$\langle \tilde{B}^*(f, \hat{\Omega}) \tilde{B}(f', \hat{\Omega}') \rangle = \frac{\delta_D^2(\hat{\Omega}, \hat{\Omega}')}{4\pi} \delta_D(f - f') \frac{P_B(f)}{2}, \quad (15)$$

Here, the shape function  $|E_{\ell}(f)|^2$  is given by [42]

$$|E_{\ell}(f)|^2 \propto \frac{1}{(f - f'_{\ell})^2 + \{f_{\ell}/(2\mathcal{Q})\}^2}, \quad (16)$$

with the eigenfrequency  $f'_{\ell}$  is the observed resonance frequency, which is slightly shifted to the one in the idealistic case,  $f_{\ell}$ , by a factor of 0.78, i.e.,  $f'_{\ell} = 0.78f_{\ell}$ , arising from several reasons including the imperfect conductivity of the Earth-ionosphere cavity. The quantity  $\mathcal{Q}$  is the so-called quality factor, for which we set  $\mathcal{Q} = 5$ , close to the one inferred from the observed spectrum of Schumann resonances (e.g., [22, 42–44]).

In Eq. (14),  $\gamma_{\ell}^B$ , which characterizes the coherence of the global magnetic field, is analytically expressed in the case of axisymmetric TM modes as follows:

$$\begin{aligned} \gamma_{\ell}^B(\hat{\mathbf{r}}_1, \hat{\mathbf{r}}_2) &= \frac{(2\ell + 1)(\ell - 1)!}{2\pi(\ell + 1)!} \\ &\times \int_{S^2} d^2\hat{\Omega} \mathcal{P}_{\ell}^1(\hat{\Omega} \cdot \hat{\mathbf{r}}_1) \mathcal{P}_{\ell}^1(\hat{\Omega} \cdot \hat{\mathbf{r}}_2) \\ &\times \{\hat{\mathbf{e}}_1(\hat{\Omega}) \cdot \hat{\mathbf{X}}_1\} \{\hat{\mathbf{e}}_2(\hat{\Omega}) \cdot \hat{\mathbf{X}}_2\}, \end{aligned} \quad (17)$$

where the function  $\mathcal{P}_{\ell}^1$  is the associated Legendre polynomials.  $\hat{\mathbf{r}}_i$  is the unit vector pointing from the earth center

to  $i$ -th detector position, and  $\hat{\mathbf{e}}_i$  points to the azimuthal direction with respect to each lightning source, is given by

$$\hat{\mathbf{e}}_i(\hat{\Omega}) = \frac{\hat{\Omega} \times \hat{\mathbf{r}}_i}{|\hat{\Omega} \times \hat{\mathbf{r}}_i|}. \quad (18)$$

The analytical model given above accounts for the magnetic noise spectrum  $M_{12}$  found in Ref. [22] through the measurement of magnetosensor, and is used in our previous paper to estimate the impact of correlated magnetic noise on the detection of stochastic GWs. We then found that for a given strength of the transfer function  $r_i(f)$ , the model can predict quantitatively the size of correlated noise, which closely match with those estimated by [23]. Nevertheless, there are oversimplification and crucial assumptions in the analytical model, which have to be tested and validated toward a realistic modeling of correlated noise. In what follows, we shall discuss one of the crucial aspects of the Schumann resonance, i.e., anisotropic distribution of lightning sources.

### III. ANISOTROPIES IN MAGNETIC FIELD SPECTRUM

In this section, relaxing the assumption of the isotropic distribution of the lightning sources in the analytical model, we discuss how the presence of anisotropic component alters the correlated noise properties.

Indeed, the distribution of lightning sources is known to be anisotropic, and rather concentrates on the continents close to the equator, associated with climate activity. Fig. 1 shows the spatial distribution of lightning activity, which is taken from the dataset of the mean annual flash rate observed by the Optical Transient Detector and the Lightning Imaging Sensor [45, 46]<sup>1</sup>. The color indicates the number of flashes per km<sup>2</sup> per year. Higher lightning activity is found at the equator of African continent. The second-generation laser interferometers, depicted as open symbols, are all located at northern hemisphere, where the lightning activity is less significant. However, due to the spatial inhomogeneities of the lightning activity, the spectrum of magnetic fields, represented as a superposition of lightning-induced magnetic fields, can become anisotropic, and thus the actual size of the impact of correlated magnetic noise would differ from each other, largely depending on their geographical location.

To see how the correlated noise properties will be changed, we extend the analytical model to incorporate the anisotropies in the magnetic field spectrum. In what follows, the magnetic field spectrum  $P_B$  defined at

<sup>1</sup> [http://lightning.nsstc.nasa.gov/data/data\\_lis-otd-climatology.html](http://lightning.nsstc.nasa.gov/data/data_lis-otd-climatology.html)

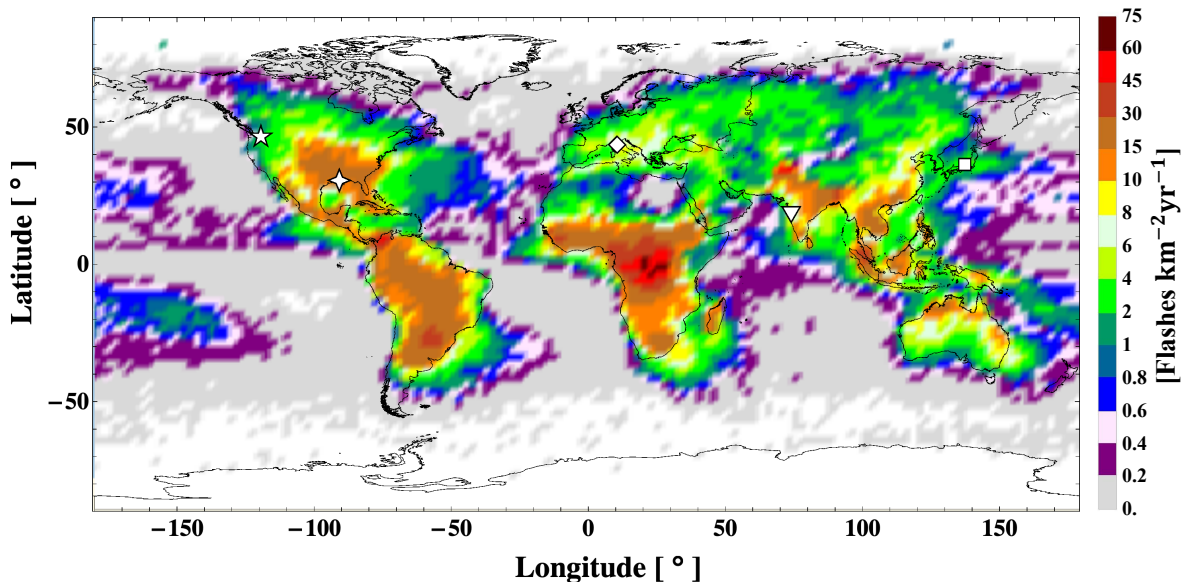


FIG. 1. World-wide density plot of mean annual flash rate with grid size of  $2.5^\circ \times 2.5^\circ$ . The color indicates the lightning flashes per  $\text{km}^2$  per year. For reference, location of the second-generation laser interferometers are indicated as open symbols: LIGO Hanford (five-pointed star), LIGO Livingston (four-pointed star), LIGO India (triangle), Virgo (diamond), and KAGRA (square).

Eq. (15) is generalized to allow anisotropic component, and is considered to be a function of not only frequency  $f$  but also angular position  $\hat{\Omega}$ , i.e.,  $P_B(f, \hat{\Omega})$ . Then, the magnetic noise spectrum,  $M_{12}$ , has to be modified, and the spectrum  $P_B$  in Eq. (14) is replaced with the sky-averaged spectrum,  $\bar{P}_B(f) = (4\pi)^{-1} \int d^2\hat{\Omega} P_B(f, \hat{\Omega})$ . The anisotropies in the magnetic field spectrum appears in the coherence function  $\gamma^B$ , which is now given by

$$\begin{aligned} \gamma_\ell^B(\hat{r}_1, \hat{r}_2) &= \frac{(2\ell+1)(\ell-1)!}{2\pi(\ell+1)!} \\ &\times \int_{S^2} d^2\hat{\Omega} \frac{P_B(f, \hat{\Omega})}{\bar{P}_B(f)} \mathcal{P}_\ell^1(\hat{\Omega} \cdot \hat{r}_1) \mathcal{P}_\ell^1(\hat{\Omega} \cdot \hat{r}_2) \\ &\times \{\hat{e}_1(\hat{\Omega}) \cdot \widehat{\mathbf{X}}_1\} \{\hat{e}_2(\hat{\Omega}) \cdot \widehat{\mathbf{X}}_2\}. \end{aligned} \quad (19)$$

That is, on top of the geometry of detector's pair and coupling parameters  $\widehat{\mathbf{X}}_i$ ,  $\gamma_\ell^B$  has an additional dependence on the anisotropies of the magnetic field spectrum.

Before going to a quantitative study in Sec. IV, it would be helpful to see how the presence of anisotropies qualitatively changes the properties of  $\gamma_\ell^B$ . Let us recall in the case of isotropic magnetic field spectrum that irrespective of geometric configuration of detector's pair, there exists a certain set of projection vectors  $\widehat{\mathbf{X}}_i$  that cancel  $\gamma_\ell^B$ . To be precise, the function  $\gamma_\ell^B$  vanishes if and only if the two projection vectors  $\widehat{\mathbf{X}}_i$  are orthogonal each other, and one of them points to the direction parallel or perpendicular to the great circle connecting the pair of detectors. In Ref. [24], we show that this nulling condition is solely due to the symmetric reason. Thus, in the

presence of anisotropies in the magnetic field spectrum, nulling condition is prone to be violated.

In Appendix A, we show that the nulling condition mentioned above still holds in the anisotropic case. However, it is only the case for a certain pair of detectors, and under the special symmetry for the magnetic field spectrum. To be precise, the magnetic field spectrum should have the axial symmetry whose symmetric axis is parallel or perpendicular to the plane spanned by detector's position vectors pointing from the earth center ( $\hat{r}_1$  and  $\hat{r}_2$ ). In other words, no global nulling condition exists, and even if one can tune the coupling parameters  $\widehat{\mathbf{X}}_i$ , the correlated noise cannot be canceled for all pairs of detectors. This indicates that the presence of anisotropies generally worsens the situation, and the impact of correlated magnetic noise on the detection of stochastic GWs become more significant.

In next section, we will see quantitatively how the impact of correlated noise sensitively depends on the anisotropies in the magnetic spectrum.

#### IV. ESTIMATION OF CORRELATED MAGNETIC NOISE FROM ANISOTROPIC LIGHTNING SOURCES

In this section, based on the observed lightning distribution shown in Fig. 1, we quantitatively estimate the impact of correlated noise on the detection of GW signal in the presence of anisotropies. After summarizing our basic setup and assumptions in Sec. IV A, we present the results in Sec. IV B.

## A. Setup

As we mentioned in Sec. I and IIB, the Schumann resonances are sourced by the lightning activity, and the spatial inhomogeneities in the lightning distribution suggests a non-negligible amount of anisotropies in the magnetic field spectrum. That is, the angular dependence of the spectrum  $P_B$  is likely to follow the lightning distribution shown in Fig. 1. Then, we introduce the parameter  $\epsilon$  that characterizes the strength of anisotropies with respect to the isotropic component. Assuming that the anisotropic component is independent of frequencies, the function  $P_B(f, \hat{\Omega})$  is expressed as

$$P_B(f, \hat{\Omega}) = \bar{P}_B(f)W(\hat{\Omega}) \quad (20)$$

with the function  $W$  given by

$$W(\hat{\Omega}) = (1 - \epsilon) + \epsilon w(\hat{\Omega}), \quad (21)$$

where the anisotropic component characterized by the function  $w$  is normalized as  $4\pi = \int d^2\hat{\Omega} w(\hat{\Omega})$ , and we assume that it simply follows the lightning distribution in Fig. 1.<sup>2</sup> For the frequency dependence of the isotropic part,  $\bar{P}_B$ , we follow the discussions in Refs. [18, 24], and adopt the power-law form:

$$\bar{P}_B(f) = A \left( \frac{f}{10\text{Hz}} \right)^{-0.88}, \quad (23)$$

with the normalization amplitude  $A^{1/2} = 5.89 \text{ pT Hz}^{-1/2}$ .

In order to estimate the impact of correlated magnetic noise, a crucial part is the strength of the coupling between laser interferometers and global magnetic fields, characterized by the transfer function  $r_i(f)$  [see Eq.(11) or (12)]. For a pair of  $i$ - and  $j$ -th detectors, the impact on stochastic GWs characterized by  $|\langle S_B \rangle|$  simply scales as  $r_i r_j$ . Here, for illustrative purpose, we consider the same functional form as used in Refs. [22–24] as a fiducial setup:

$$r_i(f) = \kappa_i \times 10^{-23} \left( \frac{f}{10\text{Hz}} \right)^{-b_i} [\text{strain pT}^{-1}], \quad (i = 1, 2). \quad (24)$$

<sup>2</sup> To be precise, Fig. 1 is given by the pixelized data set tabulated as  $(\theta_i, \phi_i, w_i)$  ( $i = 1, \dots, N$ ), where  $\theta_i$  and  $\phi_i$  are the latitude and longitude at  $i$ -th pixel, respectively, and  $w_i$  is the flash rate. Using these data, the properly normalized function  $w$  is defined as follows:

$$w(\hat{\Omega}) = 4\pi \frac{\sum_{i=1}^N w_i \delta_D(\theta - \theta_i) \delta_D(\phi - \phi_i)}{\sum_{j=1}^N w_j \sin \theta_j}. \quad (22)$$

Here, adopting the length coupling used in Ref. [22], we set the parameters  $(\kappa_i, b_i)$  to  $(2, 2.67)$  for all detectors. An updated calibration of the coupling function by Ref. [47] suggests that the amplitude of the coupling at LIGO has been substantially reduced by more than one order of magnitude in the latest instrument setup. However, the impact of correlated magnetic noise can still potentially be large for other detectors, and we still use a rather large normalization value for  $\kappa_i$ .

Based on the setup above, in what follows, we consider the five second-generation detectors, i.e., LIGO Hanford (H), Livingston (L), India (I), Virgo (V), and KAGRA (K), and estimate the impact of correlated magnetic noise, assuming the flat spectra of logarithmic energy density of stochastic GWs,  $\Omega_{\text{gw}}^A \propto f^0$ , as our fiducial target. In Appendix B, we also investigate the cases with spectral index of  $2/3$  (i.e.,  $\Omega_{\text{gw}}^A \propto f^{2/3}$ ), corresponding to the astrophysical GW background of binary coalescence [10–16]. We then compute  $|\langle S_B \rangle|$  for various detector pairs. The resultant value of  $|\langle S_B \rangle|$  is translated into the amplitude of  $\Omega_{\text{gw}} h^2$  by equating  $|\langle S_B \rangle|$  with  $S_G$ . To compute  $|\langle S_B \rangle|$  and  $\langle S_G \rangle$ , the instrumental noise spectra  $P_1$  and  $P_2$  and overlap reduction function  $\gamma_{12}^A$  involved in the optimal filter function  $\tilde{Q}$  need to be specified [see Eq. (8)]. We adopt the same noise spectral density for each detector as used in our previous paper<sup>3</sup>. The expressions for the overlap reduction function for various types of polarized GWs are analytically known, and we use them to estimate quantitatively the impact for each case<sup>4</sup>, adopting the geometrical parameters summarized in Table V of Ref. [24].

## B. Results

### 1. Correlated magnetic noise spectrum

Before presenting the quantitative impact, it would be instructive to first see how the presence of anisotropies in the magnetic field spectrum changes the behaviors of correlated magnetic noise spectrum  $M_{12}$ , which is the key quantity to estimate the cross correlation statistic in the presence of correlated noise,  $|\langle S_B \rangle|$ .

Fig. 2 shows the magnetic noise spectra  $M_{12}$  for four representative pairs of interferometers, LIGO Hanford (H), Livingston (L) and Virgo (V), and KAGRA (K) detectors. Three different lines in each upper panel represent the results with different value of  $\epsilon$ . Here, the projection vector characterizing the direction of magnetic

<sup>3</sup> For LIGO Hanford/Livingston/India, we use the table of numerical data published in Ref. [48]. For KAGRA and Virgo, we use the fitting form of the noise spectra, given at Eqs. (5) and (6) Ref. of [49], respectively.

<sup>4</sup> For unpolarized tensor, vector and scalar modes, we use the analytical form given at Eqs. (33)–(41) in Ref. [32]. For circularly polarized tensor mode, we use Eq. (8) in Ref. [40].

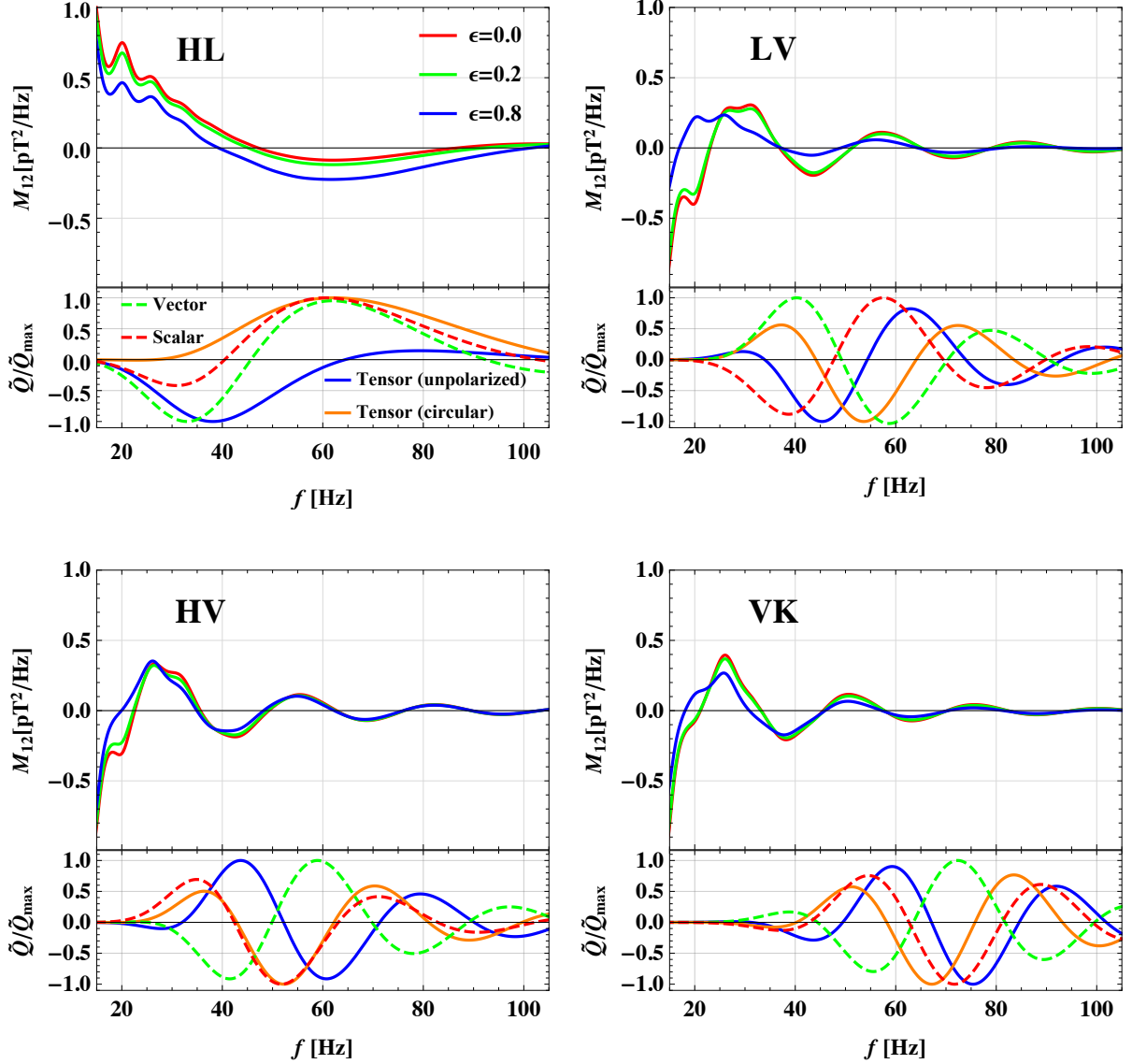


FIG. 2. Frequency dependence of magnetic noise power spectrum,  $M_{12}$  (top), and optimal filter function,  $\tilde{Q}$  (bottom), for four representative pairs: LIGO Hanford and Livingston (HL, upper left), LIGO Livingston and Virgo (LV, upper right), LIGO Hanford and Virgo (HV, lower left), and Virgo and KAGRA (VK, lower right). The response of the magnetic noise power spectrum with respect to the parameter  $\epsilon$ , which characterizes the strength of anisotropies in the magnetic field spectrum, is particularly shown in different colors. Note that the projection vector,  $\hat{X}_i$ , which describes the directional coupling to the GW detector, is chosen so that the cross correlation statistic  $|\langle S_B \rangle|$  is maximized for each pair of detectors in each value of  $\epsilon$ . The optimal filter function is computed for various types of stochastic GWs, and normalizing its amplitude by maximum value,  $\tilde{Q}_{\text{max}}$ , the results are shown in different colors and line styles.

coupling,  $\hat{X}_i$ , is chosen in such a way that the cross correlation statistic  $|\langle S_B \rangle|$  takes maximum for each pair of detector.

In Fig. 2, we also plot in each panel the optimal filter function  $\tilde{Q}$  defined at Eq. (8) for various types of stochastic GWs, normalized by its maximum amplitude  $\tilde{Q}_{\text{max}}$ . In all cases, as increasing the frequency, the op-

timal filters start to exhibit oscillatory behaviors around  $f = 20 - 100$  Hz, where the detector pair becomes sensitive to the stochastic GWs. Thus, for a non-zero  $M_{12}$  around this frequency range, a large impact of the correlated magnetic noise is expected. Fig. 2 indicates that LIGO Hanford and Livingston pair seems to be sensitively affected by the correlated magnetic noise, whereas

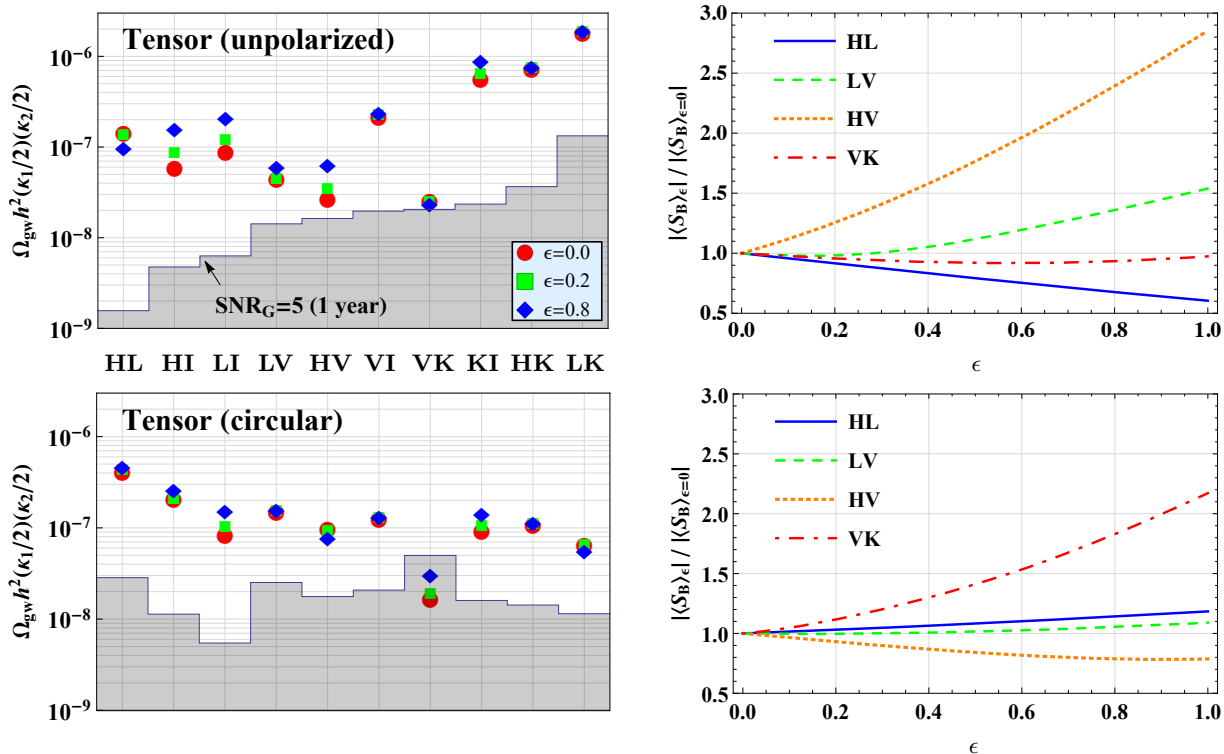


FIG. 3. *Left*: Potential impact of correlated magnetic noise on the detection of tensor GWs for  $\epsilon = 0$  (red circles), 0.2 (green squares), and 0.8 (blue diamonds). Upper panel shows the results assuming unpolarized GWs, while lower panel plots the result for circularly polarized GWs. Here, we consider the stochastic GWs with flat spectrum (i.e.,  $\Omega_{\text{gw}} \propto f^0$ ), and the cross correlation statistics  $\langle S_B \rangle$  is estimated for all possible combination of detector pairs. Then, the results are translated to  $\Omega_{\text{gw}} h^2$  by setting  $|\langle S_B \rangle| = \langle S_G \rangle$ . Note that adjusting the projection vector,  $\hat{X}_i$ , the amplitude of  $|\langle S_B \rangle|$  is maximized for each detector pair in each value of  $\epsilon$ . For reference, detectable amplitude of the stochastic GWs with signal-to-noise ratio  $\text{SNR}_G = 5$  is also estimated, assuming one-year observation. Then, the region of  $\text{SNR}_G < 5$  is shown in shaded color. *Right*: Dependence of the parameter  $\epsilon$  on the correlated magnetic noise in the presence of anisotropies in magnetic field spectrum. Normalizing their results by those in the isotropic case, we plot the ratio  $|\langle S_B \rangle_\epsilon| / |\langle S_B \rangle_{\epsilon=0}|$  as function of  $\epsilon$ . Here, the results for four representative detector pairs are only shown for unpolarized GWs (upper) and circularly polarized GWs (lower): LIGO Hanford and Livingston (HL, blue solid), LIGO Livingston and Virgo (LV, green dashed), LIGO Hanford and Virgo (HV, orange dotted), and Virgo and KAGRA (VK, red dot-dashed).

other detector pairs look less sensitive because of the rapid oscillation of both the optimal filter and magnetic noise spectrum.

Regarding the anisotropies in the magnetic field spectrum, the changes in  $M_{12}$  are basically small and are mostly coherent over  $f = 20 - 100$  Hz in all detector pairs. Hence, we naively expect its impact on the detection of stochastic GWs to vary linearly with  $\epsilon$ , and the variation of the impact would be a factor of 2 – 3. However, in the presence of oscillatory behavior in the optimal filter function, the actual size of the impact, quantified by  $\langle S_B \rangle$ , is not always the case that we naive expect. As we will see below, depending on which type of GWs we observe, the impact can change by more than a factor of 2 – 3 for some of the detector pairs. Also, interestingly, the phase cancellation in the integrand of Eq. (12) can happen, and the impact of correlated noise could be reduced to some extent.

## 2. Impact on the detection of stochastic GWs

We now present the quantitative estimate of the impact of correlated magnetic noise varying the parameter  $\epsilon$ . Figs. 3 and 4 summarize the results for tensor and non-tensor (i.e., vector and scalar) modes, respectively. In each figure, left panels plot the expected amplitude of correlated magnetic noise in terms of  $\Omega_{\text{gw}} h^2$  for all possible pair of detectors, which linearly scales with the coupling parameter of transfer function,  $\kappa_1 \kappa_2$  [see Eq. (24)]. On the other hand, right panels of Figs. 3 and 4 plot the dependence of the parameter  $\epsilon$  on the cross correlation statistic dominated by the magnetic noise, normalized by the one in the isotropic case, i.e.,  $|\langle S_B \rangle_\epsilon| / |\langle S_B \rangle_{\epsilon=0}|$ . Here, we only show the four representative cases among all possible combinations of detector pairs: LIGO Hanford and Livingston (HL), LIGO Hanford and Virgo (HV), LIGO Livingston and Virgo (LV), and finally Virgo and KA-

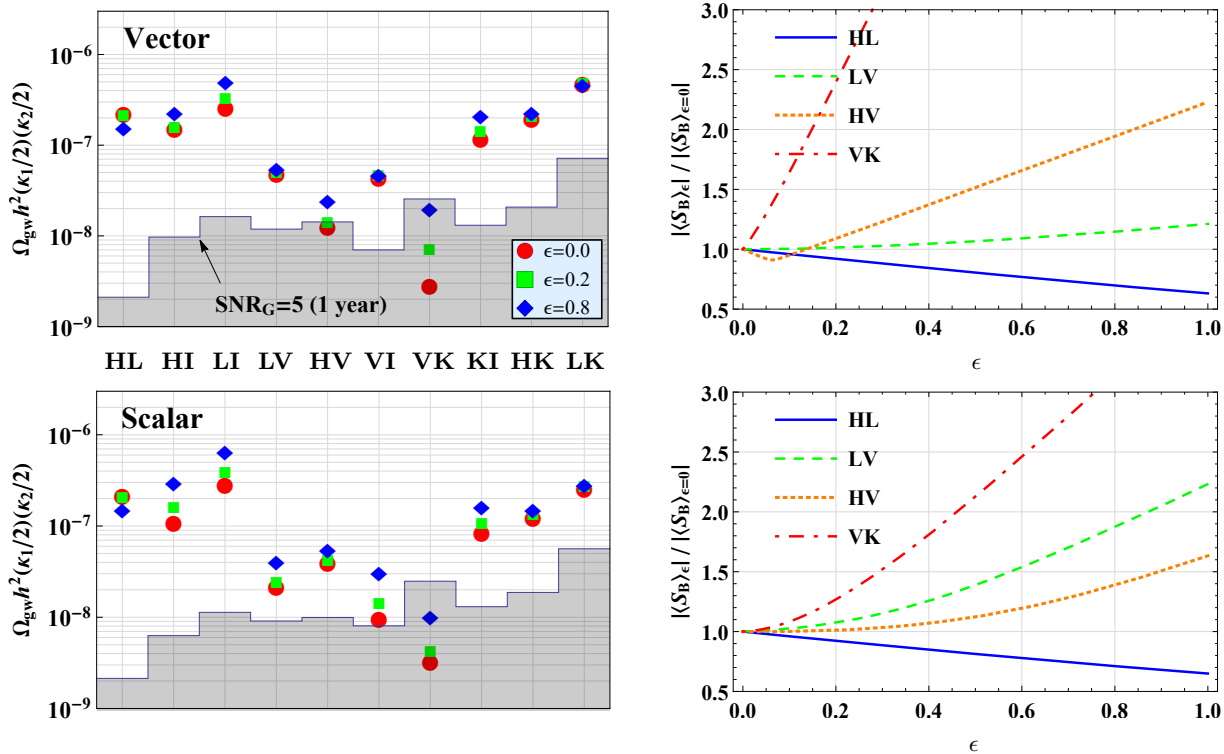


FIG. 4. Same as in Fig. 3, but in the case of vector (upper) and scalar (lower) GWs, assuming that the stochastic GWs are unpolarized.

GRA (VK). Note that all the results shown here correspond to the most pessimistic cases in the sense that the cross correlation statistic  $\langle S_B \rangle_\epsilon$  is taken to be a maximum value by adjusting the projection vectors  $\widehat{\mathbf{X}}_i$  for each pair of the detectors.

Figs. 3 and 4 basically tell us that in most of the cases, the impact of correlated magnetic noise monotonically increases with the strength of anisotropies. This is what we expected. Nevertheless, a closer look at these figures reveals several non-trivial features for specific GW mode and pairs of detectors listed below:

- For circularly-polarized tensor GWs, the variation of the amplitude,  $|\langle S_B \rangle_\epsilon$  or  $\Omega_{\text{gw}} h^2$ , with respect to  $\epsilon$  is smaller than that for other types of GWs. That is, the impact of correlated magnetic noise is mostly similar to that in the isotropic case, and it can change by a factor of 2 at maximum.
- The correlated magnetic noise at HL pair is less affected by the anisotropies in magnetic field spectrum. This is true in all types of stochastic GWs. Interestingly, for unpolarized tensor and vector/scalar GWs, relative impact on GWs gets suppressed as increasing the parameter  $\epsilon$ , although the actual impact on the detection of GWs is still large.
- VK pair is the least sensitive detector pair against the correlated magnetic noise. This is indeed the

case for all types of stochastic GWs, and for our fiducial setup, VK pair achieves the best sensitivity to the GWs among all possible pairs. Note, however, that for non-standard GWs, VK pair is largely affected by the anisotropies in the magnetic field spectrum, and the size of impact characterized by  $|\langle S_B \rangle_\epsilon|$  or  $\Omega_{\text{gw}} h^2$  can change by more than factor of 3.

These noticeable features basically come from the properties of magnetic noise spectrum and optimal filter function as we have seen in Fig. 2, and are thus ascribed to the geometrical configuration of detector pair on top of the geographical character of the lightning activity. In next section, we shall discuss this point in more detail, focusing on unpolarized tensor GWs.

## V. DISCUSSION

In this section, to better understand the results obtained in Sec. IV B, we consider the unpolarized GWs only, and examine how the geographical location of the detector pair changes the impact of correlated magnetic noise in the presence of anisotropic magnetic field spectrum. For this purpose, we artificially shift the location of detector's pair along the great circle connecting their positions, and evaluate the response of the cross correlation

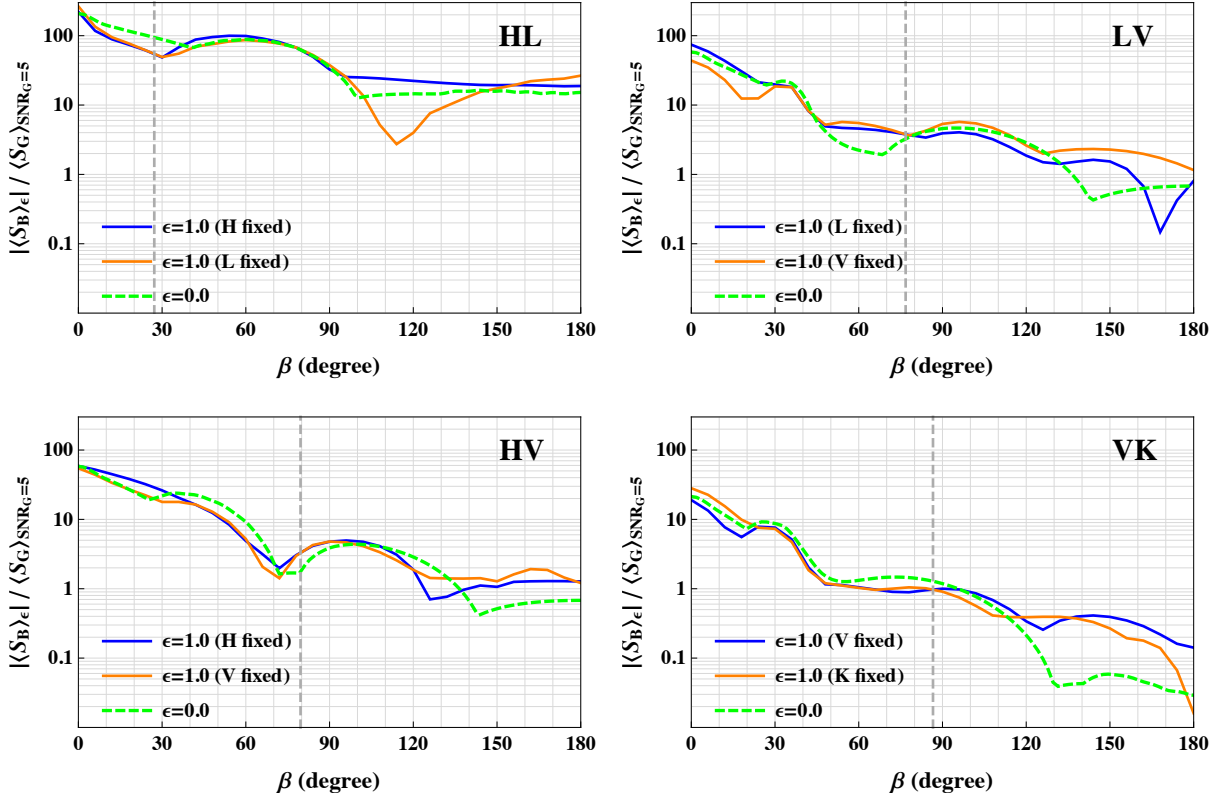


FIG. 5. Dependence of the correlated magnetic noise on the geographical setup for representative pairs of detectors: LIGO Hanford and Livingston (HL, upper left), LIGO Livingston and Virgo (LV, upper right), LIGO Hanford and Virgo (HV, lower left), and Virgo and KAGRA (VK, lower right). In each panel, shifting the location of detector’s pair along the great circle connecting their positions, we first compute the cross correlation statistic  $|\langle S_B \rangle|$ . The results are then normalized by the stochastic GW signal,  $\langle S_G \rangle$ , computed with the same setup, and are plotted as function of separation angle,  $\beta$ , defined by  $\beta \equiv \cos^{-1}(\hat{\mathbf{r}}_1 \cdot \hat{\mathbf{r}}_2)$ , where the unit vector  $\hat{\mathbf{r}}_i$  points to the  $i$ -th detector position from the earth center. Dashed lines represent the results for  $\epsilon = 0$  (i.e., isotropic case), whereas solid lines are the cases with  $\epsilon = 1$ , fixing one of the detector’s position as indicated by the figure legend. Note that in computing  $|\langle S_B \rangle|$ , the projection vectors  $\hat{\mathbf{X}}_i$  are chosen in each pair so as to maximize  $|\langle S_B \rangle|$  in the  $\epsilon = 0$  case. For reference, the vertical dashed lines indicate the separation angle of the original setup.

statistic  $\langle S_B \rangle_\epsilon$  to the variation of detector’s separation. To be precise, we fix the position for one of the detector pair to the original location, and one another position is shifted along the great circle<sup>5</sup>. Then, we compute  $\langle S_B \rangle_\epsilon$ , and the results are plotted as function of separation angle,  $\beta$ , defined by  $\beta \equiv \cos^{-1}(\hat{\mathbf{r}}_1 \cdot \hat{\mathbf{r}}_2)$ , with the unit vector  $\hat{\mathbf{r}}_i$  pointing to the  $i$ -th detector position from the earth center. Note that in computing  $\langle S_B \rangle_\epsilon$ , the directional coupling vector  $\hat{\mathbf{X}}_i$  is chosen in such a way that  $\langle S_B \rangle_\epsilon$  takes maximum value in the  $\epsilon = 0$  case.

Fig. 5 shows the results for the four representative pairs: LIGO Hanford and Livingston (HL), LIGO Livingston and Virgo (LV), LIGO Hanford and Virgo (HV), and Virgo and KAGRA (VK). Here, the correlated magnetic noise,  $|\langle S_B \rangle_\epsilon|$ , is normalized in each case by the

cross correlation statistic of the stochastic GW signals,  $\langle S_G \rangle$ , whose amplitude is determined by the signal-to-noise ratio of  $\text{SNR}_G = 5$  (see Eq. (6) for definition). A couple of notable trends is then summarized as follows:

- Overall, the impact of correlated magnetic noise, characterized by the ratio  $|\langle S_B \rangle_\epsilon| / \langle S_G \rangle_{\text{SNR}_G=5}$ , decreases as increasing the separation angle  $\beta$ , but it is not monotonically changed.
- At some separations, we see a large variation of the ratio with respect to the parameter  $\epsilon$ , and the differences between the ratios depicted as green and blue or orange lines become eventually significant.
- The anisotropies in magnetic noise spectrum, characterized by  $\epsilon$ , does not always worsen the impact of correlated magnetic noise, and the results in the isotropic case (green dashed lines) sometimes go below the blue or orange curves of  $\epsilon = 1$ .

<sup>5</sup> In this treatment, the orientation of detector pair also remains unchanged with respect to the great circle.

These trends are exactly what we have seen in Sec. IV B 2. Hence, in the presence of anisotropies in the magnetic field spectrum, the impact of correlated magnetic noise crucially depends not only on the geometric configuration, but also on the geographical locations for a pair of detectors.

Finally, we note that the VK pair tends to have a smaller value of the ratio,  $|\langle S_B \rangle_\epsilon| / \langle S_G \rangle_{\text{SNR}_G=5}$ , than others, as shown in Fig. 5. Recalling the fact that the denominator of the ratio, i.e.,  $\langle S_G \rangle_{\text{SNR}_G=5}$ , is recast as  $5\sigma$  and it is basically determined by the convolution of the noise spectral density at each detector [see Eq. (7) with optimal filter given at Eq. (8)], a smaller value of the ratio is partly ascribed to the low sensitivity to the GWs. In fact, in the original separation of detector's pair, the cross correlation amplitude  $\langle S_G \rangle_{\text{SNR}_G=5}$  for VK pair is smaller than that for HL pair by a factor of 13. However, the numerator of the ratio, i.e.,  $\langle S_B \rangle$ , for VK pair is found to be much smaller than that for HL pair over various values of  $\beta$ , and its difference amounts to a factor of 700 in the original setup. This means that for VK pair, a large cancellation happens in the integral of  $\langle S_B \rangle$ . Since the integrand is expressed as the product of the two oscillating functions, i.e.,  $M_{12}$  and  $\tilde{Q}$ , we conclude that a large cancellation basically comes from the multiple factors, including detector's characteristic, geometric reasons, as well as the properties of underlying GW signal.

## VI. CONCLUSION

According to the event rate inferred from the currently detected gravitational waves (GWs), we will be soon able to detect, via the second-generation detectors, many unresolved GW signals, viewed as a stochastic GW. Such an astrophysical origin, if detected, provides hints and clues for the formation and evolution of cosmological black hole or neutron star binaries. Increasing the sensitivity of laser interferometers, however, the correlated noise, detector's noise coupled with environmental disturbances that has global correlation, is a potential concern, and can give a large impact on the detection of stochastic GWs.

In this paper, we have presented a comprehensive study of the impact of correlated noise at low-frequency bands, which appears through the coupling of mirror control system with the stationary electro-magnetic fields on the Earth, known as the Schumann resonances. In previous work, we have proposed a simple analytical model that can characterize the impact of correlated magnetic noise on the detection of stochastic GWs. Albeit several simplifications and assumptions, the model quantitatively described the key properties of correlated magnetic noise, which indeed match with those inferred from measurement by magnetometers. Then, we have explored the possible impact of the correlated noise on the ongoing and upcoming detectors. However, one important

simplification that may possibly affect these estimates is the anisotropies in the lightning source distribution, or equivalently, the magnetic field spectrum. The present paper particularly considered this issue, and based on the observed lightning activity data, we examine if the anisotropies in the magnetic field spectrum can alter the previous estimates on the impact of correlated magnetic noise.

Introducing a model of the magnetic field spectrum given at Eq. (20) with (21), we first see that the changes in the magnetic noise spectrum,  $M_{12}$ , defined at Eq. (13), are mostly coherent and small, just in proportion to the parameter  $\epsilon$  that controls the degree of anisotropies (Sec. IV B 1). However, the quantitative estimation of the correlated magnetic noise, quantified by the cross correlation statistic  $\langle S_B \rangle$ , reveals that the impact on the detection of stochastic GWs can change largely with  $\epsilon$ , depending on which type of GWs we observe (Sec. IV B 2). As opposed to a naive expectation, the impact of correlated magnetic noise does not always increase with  $\epsilon$ , but it is rather suppressed to some extent for a specific detector's pair. One such case is LIGO Hanford and Livingston pair. Also, we find that even in the presence of anisotropies, there is a robust detector pair for which the amplitude of correlated magnetic noise becomes comparable to or well below that of the detectable stochastic GWs, irrespective of the type of GWs. This is Virgo and KAGRA pair. To better understand these results, we considered somewhat artificial situations, and found that in the presence of anisotropies, the properties of correlated magnetic noise crucially depend on both the geometrical and geographical setup of detector's pair. For Virgo and KAGRA pair, which could potentially achieve the best sensitivity to the stochastic GWs in the most pessimistic case, it is suggested that the detector's characteristic, i.e., detector's intrinsic noise property is also another important factor to reduce the impact of correlated magnetic noise.

Finally, despite several non-trivial and interesting findings in this paper, we must admit that those results may rely on the simplifications and assumptions made in our analytical model. From a conservative point of view, the results presented here have to be taken with caution. Nevertheless, the underlying reasons or explanation would be certainly relevant, and based on these, a more systematic calibration of the noise correlations have to be developed, and methodology to mitigate the correlated magnetic noise should be exploited.

## ACKNOWLEDGMENTS

This work was supported in part by MEXT/JSPS KAKENHI Grant Number JP18H04591 (YH) and JP15H05899, JP16H03977, and JP17H06359 (AT).

### Appendix A: Nulling condition for the coherence function $\gamma_\ell^B$

In this Appendix, we show that in the case of the magnetic field spectrum having a special anisotropy, there still exists the nulling condition for the coupling vectors  $\widehat{\mathbf{X}}_i$  at each detector pair, under which the coherence function  $\gamma_\ell^B$  becomes vanishing, and hence the correlated magnetic noise is canceled.

Let us first look for the nulling condition in the isotropic case (see also Ref. [24]). Substituting Eq. (18) into Eq. (17), we rewrite the coherence function  $\gamma_\ell^B$  with the following tensorial form:

$$\gamma_\ell^B(\widehat{\mathbf{r}}_1, \widehat{\mathbf{r}}_2) = \frac{(2\ell+1)(\ell-1)!}{2\pi(\ell+1)!} \times \Gamma^{be}(\ell, \widehat{\mathbf{r}}_1, \widehat{\mathbf{r}}_2) \epsilon_{abc} \epsilon_{def} \widehat{r}_1^c \widehat{r}_2^f \widehat{X}_1^a \widehat{X}_2^d, \quad (\text{A1})$$

with  $\epsilon_{abc}$  being the three-dimensional Levi-Civita symbol. Here, we adopt the Einstein's summation convention. The quantity  $\Gamma^{ab}$  is the symmetric matrix defined by

$$\Gamma^{ab}(\ell, \widehat{\mathbf{r}}_1, \widehat{\mathbf{r}}_2) = \int_{S^2} d^2\widehat{\Omega} \frac{P_\ell^1(\widehat{\Omega} \cdot \widehat{\mathbf{r}}_1)}{|\widehat{\Omega} \times \widehat{\mathbf{r}}_1|} \frac{P_\ell^1(\widehat{\Omega} \cdot \widehat{\mathbf{r}}_2)}{|\widehat{\Omega} \times \widehat{\mathbf{r}}_2|} \widehat{\Omega}^a \widehat{\Omega}^b. \quad (\text{A2})$$

Because of its rotational covariance, the above matrix is, after integrating over the solid angle, expressed as a function of  $\ell$  and the directional cosine between the position vectors  $\widehat{\mathbf{r}}_1$  and  $\widehat{\mathbf{r}}_2$ , which we denote by  $\mu \equiv \widehat{\mathbf{r}}_1 \cdot \widehat{\mathbf{r}}_2$ . We then express  $\Gamma^{ab}$  as the most general tensor form constructed with  $\delta_{ab}$  and  $\widehat{r}_a$ :

$$\Gamma^{ab}(\ell, \mu) = F_\ell(\mu) \delta^{ab} + G_\ell(\mu) (\widehat{r}_1^a \widehat{r}_2^b + \widehat{r}_2^a \widehat{r}_1^b) + H_\ell(\mu) (\widehat{r}_1^a \widehat{r}_1^b + \widehat{r}_2^a \widehat{r}_2^b). \quad (\text{A3})$$

The explicit form of the functions  $F_\ell$ ,  $G_\ell$ , and  $H_\ell$  are presented in Ref. [24], but we do not need their functional forms to find the nulling condition. Rather, we substitute Eq. (A3) into Eq. (A1), and rewrite the coherence function  $\gamma_\ell^B$  with

$$\gamma_\ell^B(\widehat{\mathbf{r}}_1, \widehat{\mathbf{r}}_2) = \frac{(2\ell+1)(\ell-1)!}{2\pi(\ell+1)!} \times \left[ F_\ell(\mu) \left\{ \mu (\widehat{\mathbf{X}}_1 \cdot \widehat{\mathbf{X}}_2) - (\widehat{\mathbf{r}}_2 \cdot \widehat{\mathbf{X}}_1) (\widehat{\mathbf{r}}_1 \cdot \widehat{\mathbf{X}}_2) \right\} - G_\ell(\mu) \left\{ (\widehat{\mathbf{r}}_1 \times \widehat{\mathbf{r}}_2) \cdot \widehat{\mathbf{X}}_1 \right\} \left\{ (\widehat{\mathbf{r}}_1 \times \widehat{\mathbf{r}}_2) \cdot \widehat{\mathbf{X}}_2 \right\} \right]. \quad (\text{A4})$$

From this expression, the coherence function is shown to be zero if the projection vectors,  $\widehat{\mathbf{X}}_i$  and  $\widehat{\mathbf{X}}_j$  ( $i, j = 1, 2$  and  $i \neq j$ ), satisfy the following relation (for any double sign):

$$(\widehat{\mathbf{X}}_i, \widehat{\mathbf{X}}_j) = \left( \pm \frac{\widehat{\mathbf{r}}_i \times \widehat{\mathbf{r}}_j}{|\widehat{\mathbf{r}}_i \times \widehat{\mathbf{r}}_j|}, \pm \frac{(\widehat{\mathbf{r}}_i \times \widehat{\mathbf{r}}_j) \times \widehat{\mathbf{r}}_j}{|(\widehat{\mathbf{r}}_i \times \widehat{\mathbf{r}}_j) \times \widehat{\mathbf{r}}_j|} \right). \quad (\text{A5})$$

Eq. (A5) is the nulling condition that cancels the correlated magnetic noise, and it says that the coherence function vanishes when the two projection vectors  $\widehat{\mathbf{X}}_i$  are orthogonal to each other, and one of them points to the direction parallel or perpendicular to the great circle connecting the pair of detectors.

Based on the nulling condition in the isotropic case, we next consider the anisotropic case, in which the coherence function is replaced with Eq. (19), and the dependence of the magnetic field spectrum appears manifest. Assuming the functional form of Eq. (20), the coherence function now depends on the function  $W(\widehat{\Omega})$ . Since this is the scalar quantity, any anisotropies in the magnetic field spectrum are expressed as the functions of  $\widehat{\Omega} \cdot \widehat{\mathbf{L}}_i$ , with  $\widehat{\mathbf{L}}_i$  being the projection vector. In principle, there must be a multiple set of projection vectors to express the general form of anisotropies. But, for illustrative purpose, we here consider the simplest case with single projection vector,  $\widehat{\mathbf{L}}$ , so that the function  $W$  is expressed in the form as  $W(\widehat{\Omega} \cdot \widehat{\mathbf{L}})$ . This means that we impose the axial symmetry in the magnetic field spectrum. Then, the symmetric matrix  $\Gamma^{ab}$  given at Eq. (A2) is replaced with

$$\Gamma^{ab}(\ell, \widehat{\mathbf{r}}_1, \widehat{\mathbf{r}}_2, \widehat{\mathbf{L}}) = \int_{S^2} d^2\widehat{\Omega} W(\widehat{\Omega} \cdot \widehat{\mathbf{L}}) \frac{P_\ell^1(\widehat{\Omega} \cdot \widehat{\mathbf{r}}_1)}{|\widehat{\Omega} \times \widehat{\mathbf{r}}_1|} \frac{P_\ell^1(\widehat{\Omega} \cdot \widehat{\mathbf{r}}_2)}{|\widehat{\Omega} \times \widehat{\mathbf{r}}_2|} \widehat{\Omega}^a \widehat{\Omega}^b. \quad (\text{A6})$$

Making use of the same analogy as in the isotropic case, the rotational covariance suggests that the above matrix is, after performing the angular integral, expressed as the function of  $\ell$ ,  $\mu$ , and  $\nu_i = \widehat{\mathbf{r}}_i \cdot \widehat{\mathbf{L}}$  ( $i = 1, 2$ ), and has the following tensorial form:

$$\Gamma^{ab}(\ell, \mu, \nu_1, \nu_2) = F_\ell \delta^{ab} + G_\ell (\widehat{r}_1^a \widehat{r}_2^b + \widehat{r}_2^a \widehat{r}_1^b) + H_\ell (\widehat{r}_1^a \widehat{r}_1^b + \widehat{r}_2^a \widehat{r}_2^b) + I_\ell \widehat{L}^a \widehat{L}^b + J_\ell (\widehat{L}^a \widehat{r}_1^b + \widehat{r}_1^a \widehat{L}^b) + K_\ell (\widehat{L}^a \widehat{r}_2^b + \widehat{r}_2^a \widehat{L}^b). \quad (\text{A7})$$

Note that all the scalar functions in the above (e.g.,  $F_\ell$ ,  $G_\ell$ ,  $H_\ell$ ,  $\dots$ ) depend not only on  $\ell$ , but also on  $\mu$ ,  $\nu_1$ , and  $\nu_2$ . Substituting Eq. (A7) into Eq. (A1), the coherence function is now given in the following form:

$$\gamma_\ell^B(\widehat{\mathbf{r}}_1, \widehat{\mathbf{r}}_2, \widehat{\mathbf{L}}) = \frac{(2\ell+1)(\ell-1)!}{2\pi(\ell+1)!} \times \left[ F_\ell \left\{ \mu (\widehat{\mathbf{X}}_1 \cdot \widehat{\mathbf{X}}_2) - (\widehat{\mathbf{r}}_2 \cdot \widehat{\mathbf{X}}_1) (\widehat{\mathbf{r}}_1 \cdot \widehat{\mathbf{X}}_2) \right\} - G_\ell \left\{ (\widehat{\mathbf{r}}_1 \times \widehat{\mathbf{r}}_2) \cdot \widehat{\mathbf{X}}_1 \right\} \left\{ (\widehat{\mathbf{r}}_1 \times \widehat{\mathbf{r}}_2) \cdot \widehat{\mathbf{X}}_2 \right\} + I_\ell \left\{ (\widehat{\mathbf{L}} \times \widehat{\mathbf{r}}_1) \cdot \widehat{\mathbf{X}}_1 \right\} \left\{ (\widehat{\mathbf{L}} \times \widehat{\mathbf{r}}_2) \cdot \widehat{\mathbf{X}}_2 \right\} + J_\ell \left\{ (\widehat{\mathbf{L}} \times \widehat{\mathbf{r}}_2) \cdot \widehat{\mathbf{X}}_2 \right\} \left\{ (\widehat{\mathbf{r}}_1 \times \widehat{\mathbf{r}}_2) \cdot \widehat{\mathbf{X}}_1 \right\} + K_\ell \left\{ (\widehat{\mathbf{L}} \times \widehat{\mathbf{r}}_1) \cdot \widehat{\mathbf{X}}_1 \right\} \left\{ (\widehat{\mathbf{r}}_1 \times \widehat{\mathbf{r}}_2) \cdot \widehat{\mathbf{X}}_2 \right\} \right]. \quad (\text{A8})$$

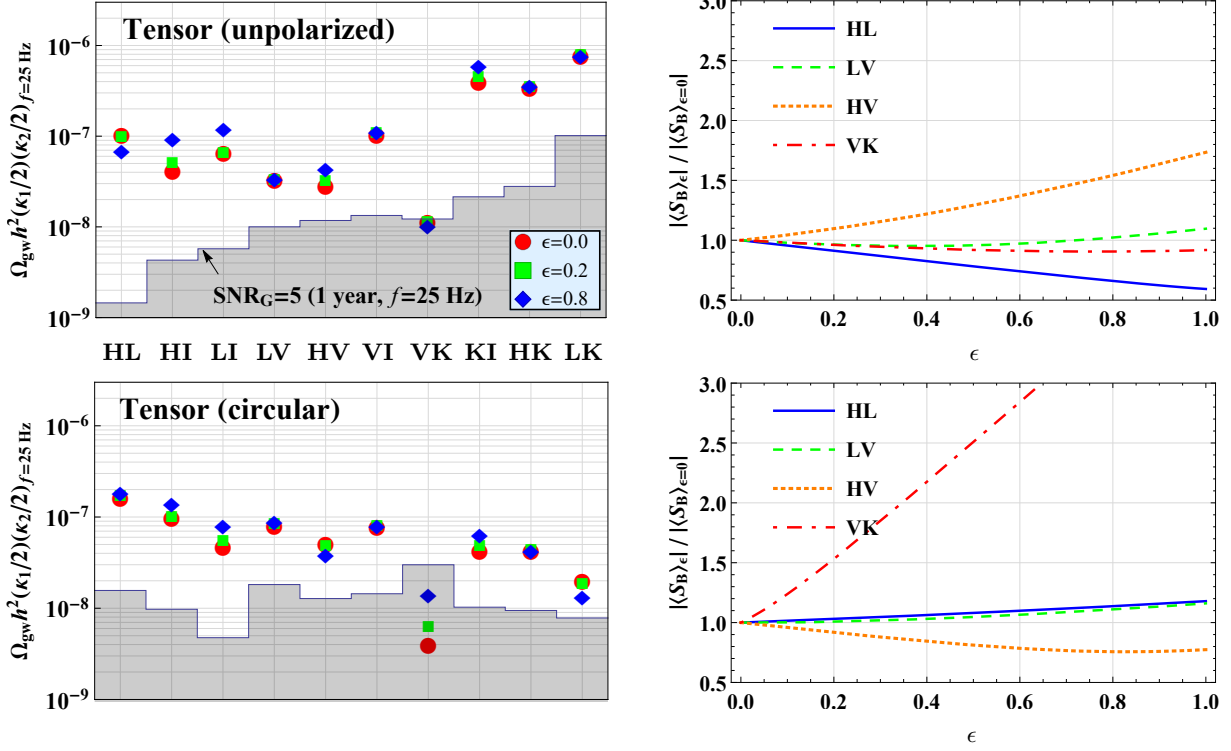


FIG. 6. Same as in Fig. 3, but here the impact of correlated magnetic noise on the detection of astrophysical GW backgrounds is shown, assuming the energy density spectrum of  $\Omega_{\text{gw}}^A \propto f^{2/3}$  with the pivot frequency  $f_0 = 25 \text{ Hz}$ , i.e.,  $\Omega_{\text{gw}}(f) = \Omega_{\text{gw},0}(f/f_0)^{2/3}$ . Then, in left panel, the estimated impact of the correlated magnetic noise is plotted as the amplitude at pivot frequency,  $\Omega_{\text{gw},0}$ .

Notice that the first two terms in the bracket are the same tensorial form as we saw in the isotropic case [see Eq. (A4)]. Thus, in order to cancel the correlated magnetic noise (equivalently to set  $\gamma_\ell^B$  to zero), the condition given at Eq. (A5) still needs to be satisfied as the sufficient condition. On top of this, the last three terms in the bracket have to be nulled, leading to the following additional constraints [substituting Eq. (A5) explicitly]:

$$(\hat{\mathbf{L}} \times \hat{\mathbf{r}}_j) \cdot \{(\hat{\mathbf{r}}_i \times \hat{\mathbf{r}}_j) \times \hat{\mathbf{r}}_j\} = 0, \quad (i, j = 1, 2 \text{ and } i \neq j), \quad (\text{A9})$$

which state that in addition to the condition for coupling vectors  $\hat{\mathbf{X}}_i$ , the symmetric axis  $\hat{\mathbf{L}}$  has to be also restricted, and it should be described by the linear combination of the vectors  $\hat{\mathbf{r}}_1$  and  $\hat{\mathbf{r}}_2$ . In other words, the symmetric axis  $\hat{\mathbf{L}}$  must lie on the plane spanned by  $\hat{\mathbf{r}}_1$  and  $\hat{\mathbf{r}}_2$ .

Note that the constraint given at Eq. (A9) does not necessarily hold for  $\hat{\mathbf{L}}$  to satisfy  $\gamma_\ell^B=0$ . In fact, one can show that the following choice is also possible, leading to  $\gamma_\ell^B = 0$  under the condition at Eq. (A5):

$$\hat{\mathbf{L}} = \frac{\hat{\mathbf{r}}_1 \times \hat{\mathbf{r}}_2}{|\hat{\mathbf{r}}_1 \times \hat{\mathbf{r}}_2|}. \quad (\text{A10})$$

That is, the symmetric axis,  $\hat{\mathbf{L}}$ , is now perpendicular to the plane spanned by  $\hat{\mathbf{r}}_1$  and  $\hat{\mathbf{r}}_2$ . Setting  $i = 1$  and  $j = 2$

in Eq. (A5) and substituting Eq. (A10) into Eq. (A8), only the term proportional to  $J_\ell$  is found to be algebraically non-vanishing. The remaining term, however, is also shown to become vanishing due to the periodicity of the integrand of  $J_\ell$  as follows. Under the conditions given at Eqs. (A5) and (A10) (with  $i = 1$  and  $j = 2$ ), we compare between the one derived from Eq. (A1) with Eq. (A6) and Eq. (A8). We obtain

$$J_\ell(\hat{\mathbf{r}}_1, \hat{\mathbf{r}}_2, \hat{\mathbf{L}}) = \frac{1}{|\hat{\mathbf{r}}_1 \times \hat{\mathbf{r}}_2| |(\hat{\mathbf{r}}_1 \times \hat{\mathbf{r}}_2) \times \hat{\mathbf{r}}_2|^2} \times \int_{S^2} d^2 \hat{\Omega} W(\hat{\Omega} \cdot \hat{\mathbf{L}}) \frac{P_\ell^1(\hat{\Omega} \cdot \hat{\mathbf{r}}_1)}{|\hat{\Omega} \times \hat{\mathbf{r}}_1|} \frac{P_\ell^1(\hat{\Omega} \cdot \hat{\mathbf{r}}_2)}{|\hat{\Omega} \times \hat{\mathbf{r}}_2|} \times \left[ \hat{\Omega} \cdot (\hat{\mathbf{r}}_2 - \mu \hat{\mathbf{r}}_1) \right] \left[ \hat{\Omega} \cdot (\hat{\mathbf{r}}_1 \times \hat{\mathbf{r}}_2) \right]. \quad (\text{A11})$$

The integrand of Eq. (A11) is the periodic function of  $\hat{\Omega}$  with respect to the rotation around the symmetric axis  $\hat{\mathbf{L}}$ , and periodically changes its sign. To see this more clearly, without loss of generality, we introduce the following coordinate system for  $\hat{\Omega}$ :

$$\hat{\Omega} = \cos \theta \hat{\mathbf{L}} + \sin \theta \left( \cos \phi \hat{\mathbf{r}}_1 + \sin \phi \hat{\mathbf{r}}_1' \right), \quad (\text{A12})$$

where  $\theta$  and  $\phi$  are the polar and azimuthal angles, respectively. The vector  $\hat{\mathbf{r}}_1'$  is the unit vector perpendicular to  $\hat{\mathbf{r}}_1$  and  $\hat{\mathbf{L}}$ , and it is expressed as  $\hat{\mathbf{r}}_1' =$

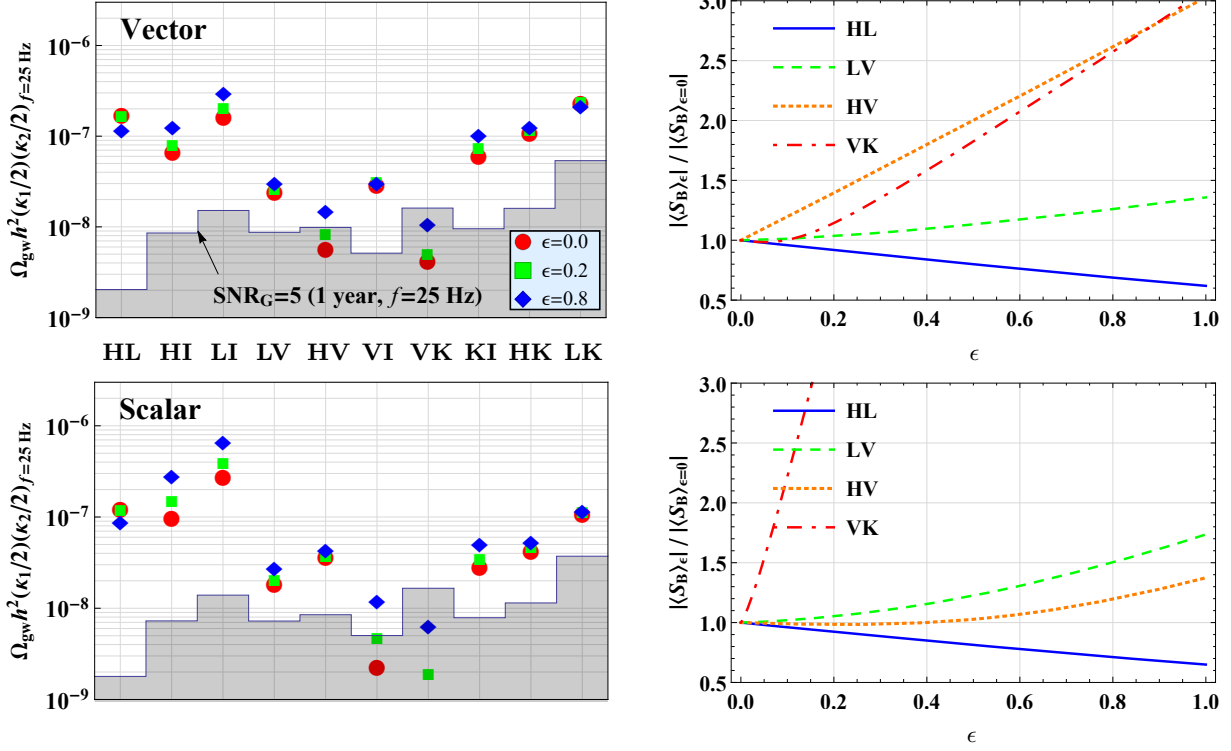


FIG. 7. Same as in Fig. 4, but here the impact of correlated magnetic noise on the detection of astrophysical GW backgrounds is shown, assuming the energy density spectrum of  $\Omega_{\text{gw}}^A \propto f^{2/3}$  with the pivot frequency  $f_0 = 25$  Hz, i.e.,  $\Omega_{\text{gw}}(f) = \Omega_{\text{gw},0}(f/f_0)^{2/3}$ . Then, in left panel, the estimated impact of the correlated magnetic noise is plotted as the amplitude at pivot frequency,  $\Omega_{\text{gw},0}$ . Note that in lower left panel, the estimated value of  $\Omega_{\text{gw},0}$  for VK pair in  $\epsilon = 0$  case is below the plotting region.

$(\hat{\mathbf{r}}_2 - \mu \hat{\mathbf{r}}_1) / \sqrt{1 - \mu^2}$ . Then, Eq. (A11) is rewritten in the following form:

$$J_\ell(\hat{\mathbf{r}}_1, \hat{\mathbf{r}}_2, \hat{\mathbf{L}}) = \frac{|\hat{\mathbf{r}}_1 \times \hat{\mathbf{r}}_2|}{|(\hat{\mathbf{r}}_1 \times \hat{\mathbf{r}}_2) \times \hat{\mathbf{r}}_2|^2} \times \int_0^\pi d\theta W(\cos\theta) \sin^2\theta \cos\theta \int_0^{2\pi} d\phi f(\theta, \phi), \quad (\text{A13})$$

with the function  $f(\theta, \phi)$  given by

$$f(\theta, \phi) = \sin\phi \frac{P_\ell^1(\sin\theta \cos\phi)}{\sqrt{\cos^2\theta + \sin^2\theta \sin^2\phi}} \frac{P_\ell^1(\sin\theta \sin(\phi + \alpha))}{\sqrt{\cos^2\theta + \sin^2\theta \cos^2(\phi + \alpha)}}. \quad (\text{A14})$$

Here, the angle  $\alpha$  is defined through the relation,  $\tan\alpha = \mu/\sqrt{1 - \mu^2}$ . Using the parity symmetry of the associated Legendre polynomials (i.e.,  $P_\ell^1(-x) = (-1)^{\ell+1} P_\ell^1(x)$ ), the function  $f$  is shown to have the following property,  $f(\theta, \phi + \pi) = -f(\theta, \phi)$ . Thus, the integral of the function  $f$  over the azimuthal angle vanishes, and hence the function  $J_\ell$  becomes zero.

## Appendix B: Impact of correlated magnetic noise on the detection of astrophysical GW backgrounds

In Sec. IV, we have estimated the impact of correlated magnetic noise assuming the stochastic GW signals with flat spectrum, i.e.,  $\Omega_{\text{gw}} \propto f^0$ . In this Appendix, we consider the stochastic GWs originated from the astrophysical sources having the power-law spectrum,  $\Omega_{\text{gw}} \propto f^{2/3}$ , and present the estimated results of the impact of correlated magnetic noise.

Similarly to Figs. 3 and 4, the estimated impact of the correlated noise,  $|\langle S_B \rangle|$ , is translated to the amplitude of stochastic GWs,  $\Omega_{\text{gw}} h^2$  at the pivot frequency  $f = 25$  Hz, and is shown in Figs. 6 and 7. Note that this frequency corresponds to the most sensitive band to detect stochastic GWs according to the design sensitivity of LIGO detectors.

Overall, qualitative trends are similar to what have been seen in Figs. 3 and 4, but the estimated values of  $\Omega_{\text{gw}} h^2$  are found to be somewhat smaller. This is basically because the signal of the stochastic GWs now comes from the higher frequency range. On the other hand, the correlated magnetic noise characterized by the magnetic noise spectrum  $M_{12}$  or coherence function  $\gamma_\ell^B$  remains unchanged, and it gives a large contribution at low frequency band. Hence, the optimal filter function involving

the underlying spectrum of stochastic GWs [see Eq. (8)] tends to pick up the higher-frequency band, and the contribution of the correlated magnetic noise is suppressed to some extent. Apart from these global trends, a couple of notable points is listed below:

- For scalar-type GWs, VI pair is less sensitive to the correlated magnetic noise, and possibly achieve the best sensitivity to the stochastic GWs, if the magnetic field spectrum is isotropic.
- In contrast to the cases with underlying stochas-

tic GWs having a flat spectrum, the correlated magnetic noise in the VK pair is rather sensitively affected by the anisotropies in the magnetic field spectrum, except for tensor-type unpolarized GWs. Nevertheless, the impact of correlated magnetic noise quantified by  $\Omega_{\text{gw}}h^2$  is well below the detectable amplitude of stochastic GWs with the signal-to-noise ratio of 5 for one-year observation (boundary between shaded and non-shaded regions), thus suggesting that VK pair is robust against correlated magnetic noise irrespective of the underlying GW signals.

- 
- [1] G. M. Harry and LIGO Scientific Collaboration, *Classical and Quantum Gravity* **27**, 084006 (2010).
- [2] LIGO Scientific Collaboration, J. Aasi, B. P. Abbott, R. Abbott, T. Abbott, M. R. Abernathy, K. Ackley, C. Adams, T. Adams, P. Addesso, and et al., *Classical and Quantum Gravity* **32**, 074001 (2015), arXiv:1411.4547 [gr-qc].
- [3] M. Maggiore, *Phys. Rep.* **331**, 283 (2000), gr-qc/9909001.
- [4] B. P. Abbott, R. Abbott, T. D. Abbott, M. R. Abernathy, F. Acernese, K. Ackley, C. Adams, T. Adams, P. Addesso, R. X. Adhikari, and et al., *Physical Review Letters* **116**, 061102 (2016), arXiv:1602.03837 [gr-qc].
- [5] B. P. Abbott, R. Abbott, T. D. Abbott, M. R. Abernathy, F. Acernese, K. Ackley, C. Adams, T. Adams, P. Addesso, R. X. Adhikari, and et al., *Physical Review Letters* **116**, 241103 (2016), arXiv:1606.04855 [gr-qc].
- [6] B. P. Abbott, R. Abbott, T. D. Abbott, M. R. Abernathy, F. Acernese, K. Ackley, C. Adams, T. Adams, P. Addesso, R. X. Adhikari, and et al., *Physical Review X* **6**, 041015 (2016), arXiv:1606.04856 [gr-qc].
- [7] B. P. Abbott, R. Abbott, T. D. Abbott, F. Acernese, K. Ackley, C. Adams, T. Adams, P. Addesso, R. X. Adhikari, V. B. Adya, and et al., *Physical Review Letters* **118**, 221101 (2017), arXiv:1706.01812 [gr-qc].
- [8] B. P. Abbott, R. Abbott, T. D. Abbott, F. Acernese, K. Ackley, C. Adams, T. Adams, P. Addesso, R. X. Adhikari, V. B. Adya, and et al., *Astrophysical Journal* **851**, L35 (2017), arXiv:1711.05578 [astro-ph.HE].
- [9] B. P. Abbott, R. Abbott, T. D. Abbott, F. Acernese, K. Ackley, C. Adams, T. Adams, P. Addesso, R. X. Adhikari, V. B. Adya, and et al., *Physical Review Letters* **119**, 141101 (2017), arXiv:1709.09660 [gr-qc].
- [10] B. P. Abbott, R. Abbott, T. D. Abbott, F. Acernese, K. Ackley, C. Adams, T. Adams, P. Addesso, R. X. Adhikari, V. B. Adya, and et al., *Physical Review Letters* **120**, 091101 (2018), arXiv:1710.05837 [gr-qc].
- [11] T. Regimbau, *Research in Astronomy and Astrophysics* **11**, 369 (2011), arXiv:1101.2762.
- [12] X.-J. Zhu, E. Howell, T. Regimbau, D. Blair, and Z.-H. Zhu, *ApJ* **739**, 86 (2011), arXiv:1104.3565 [gr-qc].
- [13] P. A. Rosado, *Phys. Rev. D* **84**, 084004 (2011), arXiv:1106.5795 [gr-qc].
- [14] S. Marassi, R. Schneider, G. Corvino, V. Ferrari, and S. Portegies Zwart, *Phys. Rev. D* **84**, 124037 (2011), arXiv:1111.6125.
- [15] X.-J. Zhu, E. J. Howell, D. G. Blair, and Z.-H. Zhu, *Mon. Not. R. Astron. Soc* **431**, 882 (2013), arXiv:1209.0595 [gr-qc].
- [16] I. Kowalska-Leszczynska, T. Regimbau, T. Bulik, M. Dominik, and K. Belczynski, *Astron. Astrophys.* **574**, A58 (2015), arXiv:1205.4621.
- [17] N. Christensen, *Phys. Rev. D* **46**, 5250 (1992).
- [18] B. Allen and J. D. Romano, *Phys. Rev. D* **59**, 102001 (1999), gr-qc/9710117.
- [19] W. O. Schumann, *Zeitschrift Naturforschung Teil A* **7**, 149 (1952).
- [20] W. O. Schumann, *Zeitschrift Naturforschung Teil A* **7**, 250 (1952).
- [21] I. Kowalska-Leszczynska, M.-A. Bizouard, T. Bulik, N. Christensen, M. Coughlin, M. Gołkowski, J. Kubisz, A. Kulak, J. Młynarczyk, F. Robinet, and M. Rohde, *Classical and Quantum Gravity* **34**, 074002 (2017), arXiv:1612.01102 [astro-ph.IM].
- [22] E. Thrane, N. Christensen, and R. M. S. Schofield, *Phys. Rev. D* **87**, 123009 (2013), arXiv:1303.2613 [astro-ph.IM].
- [23] E. Thrane, N. Christensen, R. M. S. Schofield, and A. Effler, *Physical Review D* **90**, 023013 (2014), arXiv:1406.2367 [astro-ph.IM].
- [24] Y. Himemoto and A. Taruya, *Phys. Rev. D* **96**, 022004 (2017), arXiv:1704.07084 [astro-ph.IM].
- [25] B. P. Abbott, R. Abbott, T. D. Abbott, M. R. Abernathy, F. Acernese, K. Ackley, C. Adams, T. Adams, P. Addesso, R. X. Adhikari, and et al., *Physical Review Letters* **118**, 121101 (2017), arXiv:1612.02029 [gr-qc].
- [26] F. Acernese, M. Agathos, K. Agatsuma, D. Aisa, N. Allemandou, A. Allocca, J. Amarni, P. Astone, G. Balestri, G. Ballardin, and et al., *Classical and Quantum Gravity* **32**, 024001 (2015), arXiv:1408.3978 [gr-qc].
- [27] K. Somiya, *Classical and Quantum Gravity* **29**, 124007 (2012), arXiv:1111.7185 [gr-qc].
- [28] M. W. Coughlin, A. Cirone, P. Meyers, S. Atsuta, V. Boschi, A. Chincarini, N. L. Christensen, R. De Rosa, A. Effler, I. Fiori, M. Gołkowski, M. Guidry, J. Harms, K. Hayama, Y. Kataoka, J. Kubisz, A. Kulak, M. Laxen, A. Matas, J. Młynarczyk, T. Ogawa, F. Paoletti, J. Salvador, R. Schofield, K. Somiya, and E. Thrane, *Phys. Rev. D* **97**, 102007 (2018), arXiv:1802.00885 [gr-qc].
- [29] C. S. Unnikrishnan, *International Journal of Mod-*

- ern Physics D **22**, 1341010 (2013), arXiv:1510.06059 [physics.ins-det].
- [30] A. V. Shvets, M. Hayakawa, M. Sekiguchi, and Y. Ando, Journal of Atmospheric and Solar-Terrestrial Physics **71**, 1405 (2009).
- [31] A. Shvets and M. Hayakawa, Surveys in Geophysics **32**, 705 (2011).
- [32] A. Nishizawa, A. Taruya, K. Hayama, S. Kawamura, and M.-A. Sakagami, Phys. Rev. D **79**, 082002 (2009), arXiv:0903.0528 [astro-ph.CO].
- [33] D. M. Eardley, D. L. Lee, A. P. Lightman, R. V. Wagoner, and C. M. Will, Physical Review Letters **30**, 884 (1973).
- [34] D. M. Eardley, D. L. Lee, and A. P. Lightman, Phys. Rev. D **8**, 3308 (1973).
- [35] C. M. Will, Living Reviews in Relativity **17**, 4 (2014), arXiv:1403.7377 [gr-qc].
- [36] S. H. Alexander, M. E. Peskin, and M. M. Sheikh-Jabbari, Physical Review Letters **96**, 081301 (2006), hep-th/0403069.
- [37] M. Satoh, S. Kanno, and J. Soda, Phys. Rev. D **77**, 023526 (2008), arXiv:0706.3585.
- [38] A. Nishizawa, A. Taruya, and S. Kawamura, Phys. Rev. D **81**, 104043 (2010), arXiv:0911.0525 [gr-qc].
- [39] N. Seto, Phys. Rev. D **75**, 061302 (2007), astro-ph/0609633.
- [40] N. Seto and A. Taruya, Physical Review Letters **99**, 121101 (2007), arXiv:0707.0535.
- [41] N. Seto and A. Taruya, Phys. Rev. D **77**, 103001 (2008), arXiv:0801.4185.
- [42] J. D. Jackson, *Classical Electrodynamics, 3rd Edition, by John David Jackson, pp. 832. ISBN 0-471-30932-X. Wiley-VCH, July 1998.* (Wiley, 1998) p. 832.
- [43] D. D. Sentman, Journal of Atmospheric and Terrestrial Physics **45**, 55 (1983).
- [44] C. Price, O. Pechony, and E. Greenberg, Journal of Lightning Research **1**, 1 (2007).
- [45] D. J. Cecil, D. E. Buechler, and R. J. Blakeslee, Atmospheric Research **135**, 404 (2014).
- [46] R. I. Albrecht, S. J. Goodman, D. E. Buechler, R. J. Blakeslee, and H. J. Christian, Bulletin of the American Meteorological Society **97**, 2051 (2016).
- [47] A. Effler, <https://alog.ligo-la.caltech.edu/aLOG/index.php?callRep=17851> (2015).
- [48] D. Shoemaker, <https://dcc.ligo.org/LIGO-T0900288-v3/public> (2010).
- [49] A. Manzotti and A. Dietz, arXiv e-prints (2012), arXiv:1202.4031 [gr-qc].